

Rietveld analysis of dicalcium aluminate ($\text{Ca}_2\text{Al}_2\text{O}_5$)—A new high pressure phase with the Brownmillerite-type structure

VOLKER KAHLBERG,¹ REINHARD X. FISCHER,¹ AND CLIFF S.J. SHAW²

¹Fachbereich Geowissenschaften (Kristallographie), Universität Bremen, Klagenfurter Strasse, D-28359 Bremen, Germany

²Bayerisches Geoinstitut, Universität Bayreuth, D-95440 Bayreuth, Germany

ABSTRACT

Dicalcium aluminate ($\text{Ca}_2\text{Al}_2\text{O}_5$) was prepared in a piston cylinder apparatus at 1250 °C and 2.5 GPa. The compound is orthorhombic with space group symmetry $I2mb$, $a = 5.2281(1)$ Å, $b = 14.4686(2)$ Å, $c = 5.4004(1)$ Å ($Z = 4$, $D_{\text{calc}} = 3.481$ g/cm³), and belongs to the brownmillerite structure family. Main building units are (1) layers of perovskite type corner connected AlO_6 -octahedra perpendicular to [010], and (2) zweier single chains of AlO_4 -tetrahedra running parallel [100]. The alternate stacking of the layers and sheets of single chains results in a three dimensional network in which the calcium ions are incorporated for charge compensation. The present structure is the first example for an alkaline earth aluminate with zweier single chains of tetrahedra.

INTRODUCTION

Since Hansen et al. (1928) studied the ternary system $\text{CaO-Al}_2\text{O}_3\text{-Fe}_2\text{O}_3$ the solid solution series $\text{Ca}_2\text{Fe}_2\text{O}_5\text{-Ca}_2\text{Al}_2\text{O}_5$ ($\text{C}_2\text{F-C}_2\text{A}$ using the nomenclature of cement chemistry) has been the subject of many detailed phase analytical and structural investigations (Bertaut et al. 1959; Smith 1962; Pobell and Wittmann 1965; Berggren 1971; Colville and Geller 1972). In addition to material scientific studies, brownmillerite type compounds have been recently investigated by geoscientists. For example, the defect clustering in oxygen deficient CaTiO_3 perovskites resulting from the substitution $2\text{Ti}^{4+} + \text{O}^{2-} \leftrightarrow 2\text{Fe}^{3+} + \square$ with $\text{CaFeO}_{2.5}$ as a limiting case has been studied by Becerro et al. (1999). The behavior of the oxygen vacancies and their influence on the physical properties in this model system is an important source of information on the behavior of silicate perovskites, which are thought to be a major component of the Earth's lower mantle.

According to Taylor (1997), the solid solution series $\text{Ca}_2(\text{Fe}_{1-x}\text{Al}_x)_2\text{O}_5$ exists at ordinary pressures in the compositional range between $x = 0$ and $x = 0.7$. The phases belong to two different space group types. The Fe rich compositions up to $x = 0.29$ adopt space group $Pnma$, whereas the samples beyond $x = 0.29$ crystallize in space group $I2mb$. The pure aluminum end-member C_2A ($x = 1.0$) first described by Aggarwal et al. (1972) can be prepared at high pressures only, but it can be readily preserved at ambient pressure conditions. The crystals obtained by Aggarwal and co-workers were too small for X-ray single crystal investigations. However, selected-area electron diffraction indicated that the material has an orthorhombic body centred Bravais lattice with $a = 5.24$ Å, $b = 14.40$ Å, and $c = 5.44$ Å. Structural analyses have not been performed on this high pressure phase and therefore, we decided to re-inves-

tigate this compound as part of our program on brownmillerite type material.

EXPERIMENTAL METHODS

Sample preparation

CaCO_3 (Merck, 99%) and Al_2O_3 (Aldrich, 99.8%) corresponding to the molar ratio 2:1 were used as starting materials. The reagents were carefully mixed in an agate mortar under acetone and pressed into discs (10 mm diameter and 1 mm thickness) under a pressure of 6×10^4 Pa. The pellets confined in a platinum crucible were precalcined at 1000 °C in air using a resistance heated furnace and subsequently sintered twice at 1250 °C for 24 h with intermediate grindings before final quenching in air.

Preliminary X-ray powder diffraction of the material obtained from the solid state reactions showed only two phases to be present: $\text{Ca}_3\text{Al}_2\text{O}_6$ (ICDD entry 38-1429) and $\text{Ca}_{12}\text{Al}_{14}\text{O}_{33}$ (ICDD entry 09-413).

The sintered precursor material was re-ground and used for high pressure experiments which were performed at the Bayerisches Geoinstitut choosing the same temperature and pressure conditions as described in Aggarwal et al. (1972). The experiments were accomplished in a 1/2 inch piston cylinder apparatus using talc pyrex cells with a tapered graphite heater. The samples were encapsulated in 1 cm long and 5 mm diameter welded Pt capsules. The experiments were performed at 2.5 GPa and 1250 °C for 2 h. Pressure was calibrated against the quartz-coesite and kyanite-sillimanite transitions as well as the melting point of diopside. A friction correction of 18% was applied to the nominal pressure on the basis of these calibration data. Temperature was measured with a $\text{Pt}_{90}\text{Rh}_{10}$ -Pt thermocouple and controlled with a Eurotherm 818 controller. Temperatures are considered to be accurate within ± 10 °C with a temperature gradient of about 5 °C from the top to the middle

*E-mail: vkahlen@zfn.uni-bremen.de

of the capsule (Shaw and Fliervoet, unpublished data). The experiments were carried out using the hot-piston out technique. The samples were quenched isobarically by turning off the power of the furnace. Quench rates were of the order of 75 °C/s.

Powder diffraction data analysis

Due to the small amounts of material obtained from the high pressure experiments, the data collection for the structure analysis was performed on a Stoe STADI-P diffractometer in flat plate transmission geometry. The diffractometer is equipped with a curved Ge monochromator in the primary beam yielding a strictly monochromatic $\text{CuK}\alpha_1$ -radiation. The sample was prepared between two thin foils and fixed with silicone grease (Baysilone). The effective value for the product μt (μ = linear absorption coefficient; t = sample thickness) used for the absorption correction was determined experimentally from the intensity ratios at $\theta = 0^\circ$ with and without the sample. Details of the data collection, crystallographic data and definitions are given in Table 1.

A first inspection of the X-ray diffraction pattern revealed that all peaks could be indexed on the basis of an orthorhombic cell close to the one reported by Aggarwal et al. (1972). There was no indication of additional reflections from the starting material. For the Rietveld analysis the background was set by hand, because it could not be described by a simple function because of its irregular shape due to the scattering of the grease

used for fixing the sample. Background values were determined by linear interpolation between consecutive breakpoints in the pattern. Intensities within eight times the full width at half maximum of a peak were considered to contribute to the central reflexion. Peaks below $2\theta = 15^\circ$ were corrected for asymmetry effects after Rietveld (1969). The pseudo-Voigt function was chosen for the simulation of the peak shape, with two parameters defining the Lorentzian and Gaussian character of the peaks as a function of 2θ . The angular variation of the line width was accounted for by using the Cagliotti function (Cagliotti et al. 1958). The powder diffraction data for $\text{Ca}_2\text{Al}_2\text{O}_5$ including calculated (based on the unit cell parameters of the Rietveld analysis), observed peak positions, and relative background corrected intensities are listed in Table 2. The figures of merit

TABLE 1. Experimental conditions and crystallographic data

Radiation type, source	X-ray, $\text{CuK}\alpha_1$
Generator settings	40 KV, 40 mA
Discriminator	primary beam, curved Ge (111)
Detector	monochromator linear PSD
Secondary soller slit width	1 mm
Effective (μt)	1.40
Data collection temperature	room temperature
Range in 2θ	5.0–130°
Step size	0.01°
Counting time per step	240 s
Space group	$I2mb$
Chemical composition	$\text{Ca}_2\text{Al}_2\text{O}_5$
Z	4
Lattice parameters (Å)	<i>a</i> 5.2281(1) <i>b</i> 14.4686(2) <i>c</i> 5.4004(1)
No. steps	12500
No. contributing reflections	205
No. structural parameters	22
No. profile parameters	8
R_{wp} (%)	8.6
R_p (%)	20.2
R_B (%)	6.8

Notes:

$$R_{wp} = \sqrt{\frac{\sum_i w_i (y_{io} - C \cdot y_{ic})^2}{\sum_i w_i y_{io}^2}}; R_p = \frac{\sum_i |y_{io} - C \cdot y_{ic}|}{\sum_i |y_{io} - y_{ic}|}; R_B = \frac{\sum_k |I_{ko} - C \cdot I_{kc}|}{\sum_k I_{ko}}$$

y_o, y_c = observed and calculated profile intensities; I_o, I_c = observed and calculated integrated intensities; C = Scaling factor; w = weight = $1/y_o$. Standard deviations for the lattice constants are given in parentheses.

TABLE 2. X-ray powder diffraction data for $\text{Ca}_2\text{Al}_2\text{O}_5$

<i>h k l</i>	$2\theta_{\text{obs}}$	$2\theta_{\text{calc}}$	d_{obs}	d_{calc}	Intensity
0 2 0	12.211	12.224	7.242	7.235	31
0 1 1	17.521	17.514	5.057	5.060	5
1 0 1	23.661	23.667	3.757	3.756	4
0 3 1	24.730	24.729	3.597	3.597	21
1 2 1	26.718	26.719	3.334	3.334	9
0 0 2	33.141	33.150	2.701	2.700	44
2 0 0	34.272	34.275	2.614	2.614	69
1 4 1	34.386	34.391	2.606	2.606	100
0 5 1	35.146	35.155	2.551	2.551	14
0 2 2	35.422	35.455	2.532	2.530	1
2 2 0	36.508	36.518	2.459	2.459	3
0 6 0	37.280	37.257	2.410	2.411	1
1 1 2	37.979	37.986	2.367	2.367	3
2 1 1	38.748	38.741	2.322	2.322	1
0 4 2	41.710	41.708	2.164	2.164	25
1 3 2	42.029	42.029	2.148	2.148	2
2 4 0	42.645	42.638	2.118	2.119	24
1 6 1	44.612	44.616	2.029	2.029	29
2 0 2	48.418	48.426	1.878	1.878	52
1 5 2	49.281	49.299	1.848	1.847	3
2 5 1	49.923	49.914	1.825	1.826	4
2 2 2	50.128	50.140	1.818	1.818	14
0 8 0	50.419	50.416	1.808	1.809	20
0 6 2	50.714	50.715	1.799	1.799	7
2 6 0	51.496	51.518	1.773	1.772	5
1 0 3	53.791	53.816	1.703	1.702	1
0 3 3	54.343	54.354	1.687	1.686	8
2 4 2	55.035	55.048	1.667	1.667	1
1 2 3	55.399	55.410	1.657	1.657	1
3 2 1	56.900	56.914	1.617	1.617	2
1 7 2	58.900	58.931	1.567	1.566	3
1 4 3	60.008	60.021	1.5404	1.5401	15
0 5 3	60.512	60.523	1.5287	1.5285	3
3 4 1	61.444	61.453	1.5078	1.5076	17
0 8 2	61.659	61.676	1.5030	1.5027	6
2 8 0	62.398	62.384	1.4870	1.4873	6
3 1 2	63.879	63.843	1.4560	1.4568	2
2 3 3	65.835	65.851	1.4174	1.4171	4
1 6 3	67.257	67.275	1.3909	1.3906	5
3 6 1	68.610	68.623	1.3667	1.3665	5
1 10 1	69.557	69.572	1.3504	1.3502	9
0 2 4	70.951	70.956	1.3273	1.3272	3
4 0 0	72.222	72.220	1.3070	1.3070	6
2 8 2	72.493	72.495	1.3028	1.3027	12
4 2 0	73.546	73.579	1.2867	1.2862	2
4 4 0	77.610	77.604	1.2292	1.2292	1
2 0 4	79.868	79.903	1.2000	1.1996	1
3 7 2	80.288	80.285	1.1948	1.1948	2
2 2 4	81.224	81.220	1.1833	1.1834	3
4 0 2	81.779	81.801	1.1767	1.1765	3
2 10 2	84.430	84.449	1.1464	1.1462	3
3 6 3	87.750	87.765	1.1114	1.1112	3
3 10 1	89.913	89.901	1.0902	1.0903	2
0 10 4	102.571	102.585	0.9872	0.9871	3

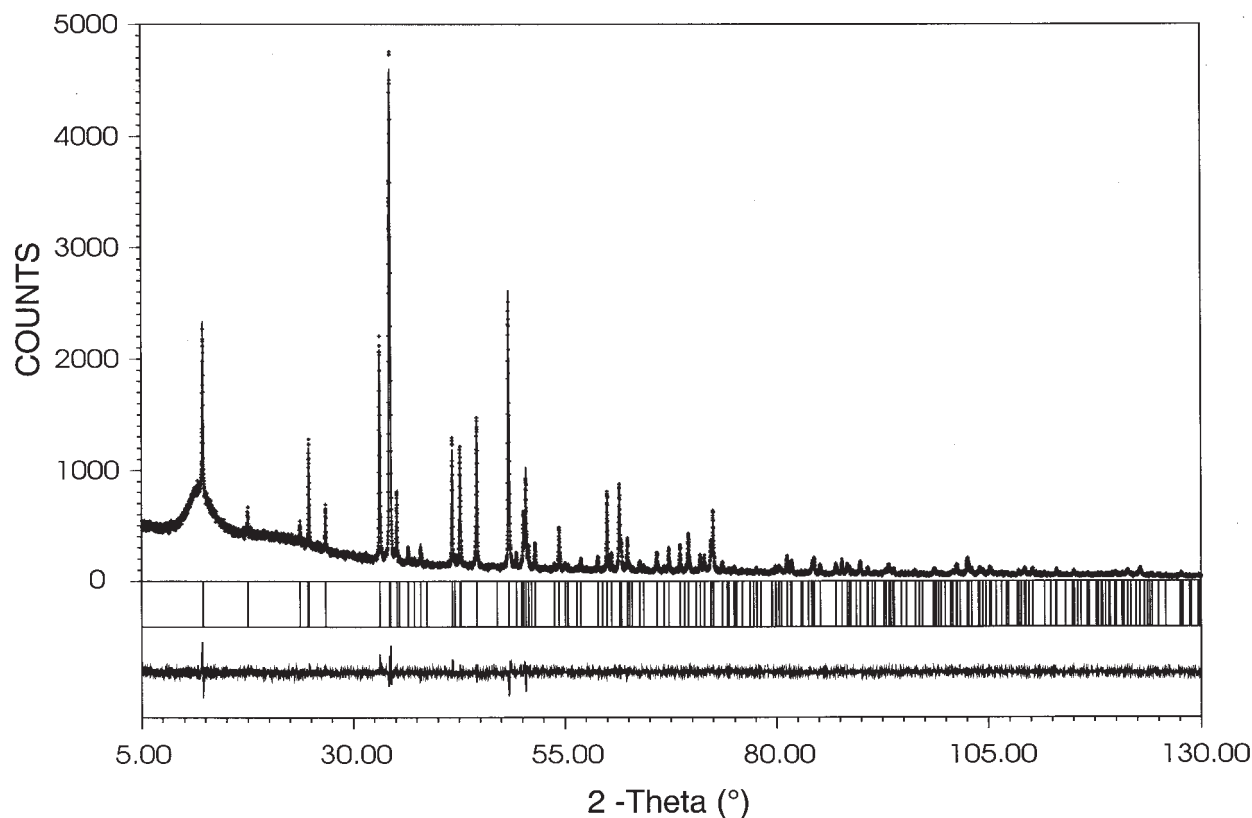


FIGURE 1. Observed (crosses) and calculated (solid line) step intensities and their difference (dotted line at bottom of figure) of $\text{Ca}_2\text{Al}_2\text{O}_5$. Peak positions permitted by the unit cell metric are indicated by tick marks (middle portion).

M_{20} (de Wolff 1968) and F_{30} (Smith and Snyder 1979) for assessing the quality of the indexed powder pattern of $\text{Ca}_2\text{Al}_2\text{O}_5$ are $M_{20} = 88$ and $F_{30} = 85$ (0.0098; 36).

STRUCTURE ANALYSIS AND REFINEMENT

The structure analysis as well as distance and angle calculations were performed with a modified version of the PC-Rietveld plus package (Fischer et al. 1993) adopted for transmission geometry. X-ray scattering factors in their respective valence states were taken from the *International Tables for X-ray crystallography Vol. IV* (Ibers and Hamilton 1974) and the values for O^{2-} from Hovestreydt (1983). For the drawing of the structural details, the computer programs ATOMS (Dowty 1995) and ORTEP-3 (Farrugia 1997) were used. Starting values for the fractional atomic coordinates were taken from Colville and Geller (1972) and transformed to the *I2mb* space group. This non-standard setting of space group *Ima2* (no. 46) was selected to compare the coordinates between the body centered and the primitive brownmillerite structure type (*Pnma* setting) directly, without any transformation of coordinates.

The refinement was done in consecutive steps with the atomic coordinates and the thermal parameters held fixed in the initial calculations. They were allowed to vary after the scale factor, zero point, peak shape parameters, and lattice constants were close to convergence to their optimum values. For

the final calculations a flat plate absorption correction was included. The graphical comparison between the observed and calculated powder pattern is given in Figure 1. The refined fractional atomic coordinates are listed in Table 3 and selected interatomic distances and angles in Table 4.

The two main building units of dicalcium aluminate are: (1) layers of perovskite type corner connected AlO_6 -octahedra perpendicular to [010] and (2) zweier single chains of AlO_4 -tetrahedra running parallel [100]. The alternate stacking of the layers and sheets of single chains results in a three dimensional network. Charge balance is achieved by calcium ions located in voids of the framework (compare Fig. 2).

The average value of the O-Al-O angle is very close to the ideal value of 109.4° , whereas the individual O-Al-O angles vary between 104° and 125° , respectively. This spread in the angles indicates a significant distortion of the tetrahedra and can be expressed numerically with the quadratic elongation $l = 1.014$ and the angle variance $\sigma^2 = 62.3$ as defined by Robinson et al. (1972). The individual octahedra within the perovskite type sheets are significantly less distorted ($l = 1.008$; $\sigma^2 = 8.5$). They are tilted against each other by rotations of $\pm 5^\circ$ about [100] and $\pm 1^\circ$ about [010]. Both the tetrahedra and octahedra are primarily distorted along the crystallographic *b* axis. The calcium cations are coordinated by eight neighbors forming distorted bicapped trigonal prisms.

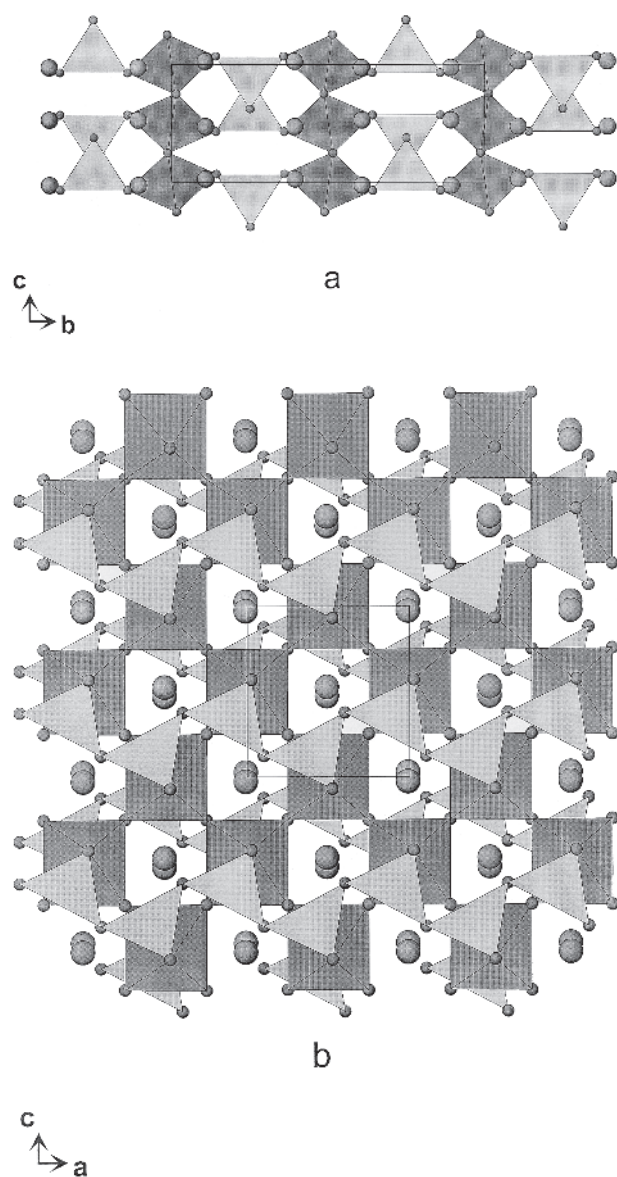


FIGURE 2. Projections of the whole structure of $\text{Ca}_2\text{Al}_2\text{O}_5$ (a) parallel to $[100]$ and (b) parallel $[010]$. The large spheres in the interstitial sites = Ca atoms; smaller spheres = O anions. Light shading = tetrahedra. Dark shading = octahedra.

COMPARISON WITH OTHER STRUCTURES

A comparison of the main structural data of the end-members of the solid solution series $\text{C}_2\text{F}-\text{C}_2\text{A}$ is given in Table 5. The trends in the mean cation-oxygen distances of the tetrahedra and octahedra are consistent with the substitution of Fe^{3+} by the smaller Al^{3+} . Furthermore, the Ca-O distances are longer for dicalcium ferrite. The intra-chain $\text{Me}^{\text{tet}}\text{-O-Me}^{\text{tet}}$ angles are definitely larger in C_2A , indicating an increased stretching of the chains in the aluminates.

The value of 125° for an tetrahedral O-Al-O angle is a con-

TABLE 3. Fractional atomic coordinates for $\text{Ca}_2\text{Al}_2\text{O}_5$ and isotropic displacement factors (\AA^2)

Atom	Position	x	y	z	B_{iso}
Al1	4a	$\frac{1}{2}$	$\frac{1}{2}$	$\frac{1}{2}$	0.83(5)
Al2	4b	0.4487(11)	$\frac{1}{4}$	0.5733(5)	0.42(7)
Ca	8c	0.4937(11)	0.6079(1)	0.9770(3)	0.64(3)
O1	8c	0.5223(14)	0.3570(2)	0.4432(6)	0.86(10)
O2	4b	0.6100(16)	$\frac{1}{4}$	0.8615(10)	1.06(16)
O3	8c	0.2590(18)	0.5090(2)	0.2560(11)	0.80(7)

TABLE 4. Selected interatomic distances (\AA) and bond angles ($^\circ$) for $\text{Ca}_2\text{Al}_2\text{O}_5$

$2\times$ Al1-O3	1.828(8)	$2\times$ O3-Al1-O3	87.85(3)
$2\times$ Al1-O3	1.940(8)	O3-Al1-O3	91.44(3)
$2\times$ Al1-O1	2.095(3)	$2\times$ O3-Al1-O3	180.00
		O3-Al1-O3	92.85(3)
		$2\times$ O1-Al1-O3	94.22(2)
		$2\times$ O1-Al1-O3	90.19(2)
		$2\times$ O1-Al1-O3	89.95(2)
		$2\times$ O1-Al1-O3	85.60(2)
		O1-Al1-O1	173.63(2)
$2\times$ Al2-O1	1.743(4)	O1-Al2-O1	125.27(3)
Al2-O2	1.770(7)	$2\times$ O2-Al2-O1	104.45(2)
Al2-O2	1.805(10)	$2\times$ O2-Al2-O1	107.15(2)
		O2-Al2-O2	107.22(3)
Ca-O2	2.314(4)	Ca-O1	2.330(4)
Ca-O3	2.413(8)	Ca-O3	2.440(8)
Ca-O3	2.460(9)	Ca-O3	2.493(9)
Ca-O1	2.523(9)	Ca-O1	2.816(9)

TABLE 5. Comparison of selected structural data for C_2F and C_2A

	$\langle \text{M}^{\text{tet}}\text{-O} \rangle$	$\langle \text{M}^{\text{oct}}\text{-O} \rangle$	$\langle \text{Ca-O} \rangle$	$\text{Me}^{\text{tet}}\text{-O-Me}^{\text{tet}}$
C_2F	1.878	2.016	2.543	123.2
C_2A	1.765	1.954	2.474	125.3

Notes: Bond distances in (\AA) and bond angles in ($^\circ$). The data for C_2F are based on the co-ordinates from Berggren (1971).

spicuous feature of this structure, being close to the upper limit of observed O-Al-O angles in alkali and alkaline earth-aluminates (compare Fig. 3). As is shown in Figure 4 this angle occurs at the O1 ligands connecting the octahedral layers and the tetrahedral chains. A shortening of the O1-O1 edge of the tetrahedron makes the angle smaller, yielding a more regular tetrahedral geometry, but stretches the Al1-O1 bond in the octahedron. Distance least squares calculations using the program DLS-76 (Baerlocher et al. 1977) with prescribed distances for all cations and anions result in atomic positions with an O1-Al2-O1 angle of 130° . Forcing the tetrahedron to assume a regular geometry by assigning a high weight to the O1-O1 bond causes a lengthening of the Al1-O1 bond in the octahedron from 2.05 \AA in the unconstrained DLS-refinement (2.09 \AA observed) to a crystal chemical unrealistic value of 2.23 \AA in the DLS-refinement with essentially fixed tetrahedral geometry.

Likewise, the Ca ions are moved toward Al1 yielding a rather short Al-Ca distance of 2.94 \AA (Al-Ca distances for all the structural characterized calcium aluminates begin at about 3.10 \AA). The relatively high DLS reliability index of 0.044 for the configuration resulting from the unconstrained refinement (essentially representing the actually observed structure) shows that

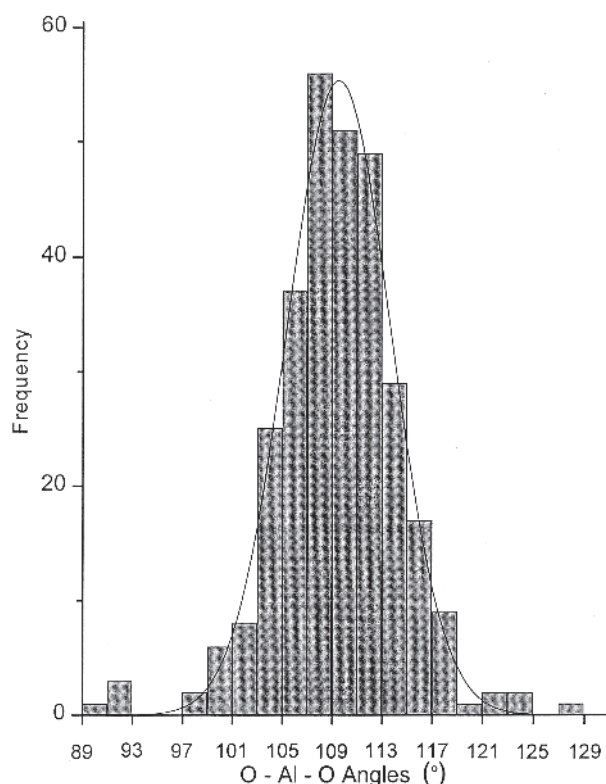


FIGURE 3. Histogram of O-Al-O angles observed in alkali and alkaline earth aluminates (300 angles; 21 different structures). The frequency distribution can be approximated by a normal distribution with maximum: 109.5° and standard deviation: 4.2° .

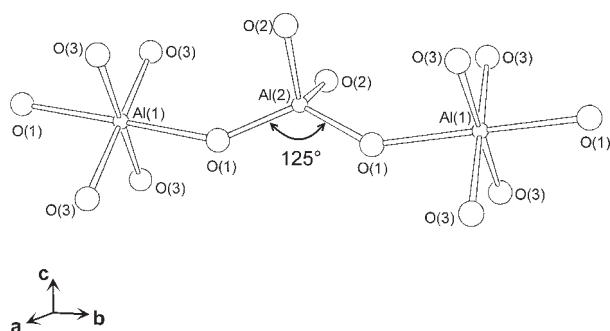


FIGURE 4. Perspective view (15° off the $[100]$ -direction) of a small part of the structure.

C_2A is considerably strained and this may explain why this brownmillerite type phase is only formed at high pressures.

$\text{Ca}_2\text{Al}_2\text{O}_5$ is one of the rare cases among the group of alkaline earth aluminates where Al^{3+} exhibits both a fourfold and sixfold coordination. Examples described in prior investigations are the two hibonite type compounds CaAl_2O_9 (Kato

and Saalfeld 1968) and SrAl_2O_9 (Lindop et al. 1975) as well as $\text{Sr}_4\text{Al}_{14}\text{O}_{25}$ (Nadezhina et al. 1976). Furthermore, dicalcium aluminate is the first example of a pure aluminate with zweier single chains of corner connected tetrahedra.

ACKNOWLEDGMENTS

We thank W. Schmidt (Max-Planck-Institut für Kohlenforschung, Mülheim / Ruhr, Germany) for collecting the powder diffraction data, and M. Kunz and a second anonymous reviewer for their helpful comments on the manuscript.

REFERENCES CITED

- Aggarwal, P.S., Gard, J.A., and Glasser, F.P. (1972) Synthesis and properties of dicalcium aluminate, $2\text{CaO}\cdot\text{Al}_2\text{O}_3$. *Cement and Concrete Research*, 2, 291–297.
- Baerlocher, C., Hepp, A., and Meier, W.M. (1977) DLS-76, a program for the simulation of crystal structures by geometric refinement. Institute of Crystallography and Petrography, ETH Zürich, Switzerland.
- Becerro, A.I., Lauterbach, S., McCammon, C.A., Langhorst, F., Angel, R., and Seifert, F. (1999) Oxygen defect clustering in $\text{CaTiO}_3\text{-CaFeO}_{2.5}$ perovskites: a model for the lower mantle. *European Journal of Mineralogy*, 11, Supplement 1, 27.
- Berggren, J. (1971) Refinement of the crystal structure of dicalcium ferrite, $\text{Ca}_2\text{Fe}_2\text{O}_5$. *Acta Chemica Scandinavica*, 25, 3616–3624.
- Bertaut, E.F., Blum, P., and Sagnières, A. (1959) Structure du ferrite bicalcique et de la brownmillerite. *Acta Crystallographica*, 12, 149–159.
- Cagliotti, G., Paoletti, A., and Ricci, F.P. (1958) Choice of collimators for a crystal spectrometer for neutron diffraction. *Nuclear Instruments*, 3, 223–228.
- Colville, A.A. and Geller, S. (1972) Crystal structures of $\text{Ca}_2\text{Fe}_{1.43}\text{Al}_{0.57}\text{O}_5$ and $\text{Ca}_2\text{Fe}_{1.28}\text{Al}_{0.72}\text{O}_5$. *Acta Crystallographica*, B28, 3196–3200.
- de Wolff, P.M. (1968) A simplified criterion for the reliability of a powder pattern indexing. *Journal of Applied Crystallography*, 1, 108–113.
- Dowty, E. (1995) *Atoms for Windows*, Version 3.2. Shape Software, 521 Hidden Valley Rd., Kingsport, Tennessee 37663.
- Farrugia, L.J. (1997) ORTEP-3 for Windows. *Journal of Applied Crystallography*, 30, 565.
- Fischer, R.X., Lengauer, C.L., Tillmanns, E., Ensink, R.J., Reiss, C.A., and Fantner, E.J. (1993) PC-Rietveld Plus, a comprehensive Rietveld analysis package for PC. *Materials Science Forum*, 133–136, 287–292.
- Hansen, W.C., Brownmiller, L.T., and Bogue, R.H. (1928) Studies on the system calcium oxide-alumina-ferric-oxide. *Journal of the American Chemical Society*, 50, 396–408.
- Hovestreydt, E. (1983) On the atomic scattering factor of O^{2-} . *Acta Crystallographica*, A39, 268–269.
- Ibers, J.A. and Hamilton, W.C., Eds. (1974) *International tables for X-ray crystallography*, vol. IV, Kynoch, Birmingham, U.K.
- Kato, K. and Saalfeld, H. (1968) Verfeinerung der Kristallstruktur von $\text{CaO}(\text{Al}_2\text{O}_3)_6$. *Neues Jahrbuch für Mineralogie, Abhandlungen*, 109, 192–200.
- Lindop, A.J., Matthews, C., and Goodwin, D.W. (1975) The refined structure of $\text{SrO}(\text{Al}_2\text{O}_3)_6$. *Acta Crystallographica*, B31, 2940–2941.
- Nadezhina, T.N., Pobedimskaya, E.A., and Belov, N.V. (1976) Crystal structure of strontium aluminate $\text{Sr}_4\text{Al}_{14}\text{O}_{25}$. *Kristallografiya*, 21, 826–828.
- Pobell, F. and Wittmann, F. (1965) Replacement of Fe^{3+} by Al^{3+} in calciumaluminate-ferrite. *Physics Letters*, 19, 175–176.
- Rietveld, H.M. (1969) A profile refinement method for nuclear and magnetic structures. *Journal of Applied Crystallography*, 2, 65–71.
- Robinson, K., Gibbs, G.V., and Ribbe, P.H. (1972) Quadratic elongation: a quantitative measure of distortion in polyhedra. *Science*, 171, 567–570.
- Smith, D. (1962) Crystallographic changes with the substitution of aluminium for iron in dicalcium ferrite. *Acta Crystallographica*, 15, 1146–1152.
- Smith, G.S. and Snyder, R.L. (1979) F(N): A criterion for rating powder diffraction patterns and evaluating the reliability of powder pattern indexing. *Journal of Applied Crystallography*, 12, 60–65.
- Taylor, H.F.W. (1997) *Cement chemistry*, Thomas Telford, London, 459 p.